
Models for Biological Motor Control: Modules of Movements

Irina Alles

Department of Computer Science
Technische Universität Darmstadt
Darmstadt, 64289
ialles@gmx.de

Abstract

This paper gives an overview of recent work in the domain of biological motor control. In particular we address the question of how the central nervous system represents and solves the transformation of a goal into the appropriate motion. Therefore we focus on studies from [dAve 05] and [Over 08] which suggest that motor control is accomplished using a modular structure of muscle activations.

1 Introduction

To illustrate the complexity of motor control let us consider a task which is accomplished by our central nervous system (CNS) every day like the transformation of a goal into an action. Taking the example of primate grasping, discussed in [Over 08] and reducing it only to the phase of a monkey's arm reaching for a specific object. This action can be achieved by an infinite number of trajectories. Each trajectory can be created by several combinations of joint motions of the corresponding parts of the body, like arm and wrist and additionally these single motions can be created by multiple muscle combinations. In order to accomplish such a task one has to solve the so called problem of "inverse dynamics"[Muss 00]. The "direct" dynamics problem is the calculation of a trajectory given a certain force, which can be achieved using integration and deriving the limbs acceleration. But the CNS must solve the inverse problem, given a planned trajectory it must calculate the required force and the appropriate muscles. Additionally taking into account that multiple combinations of muscles can result in the same torque, thus the dimensionality of the search space gets very high, also known as Degrees of Freedom (DOF) problem.

One way for the CNS to manage this complexity is to find statistical regularities in the environment and operate using these regularities rather than individual variables [Tres 06]. In the visual system this concept is applied using "features" of the environment, like edges and bars encoded in the visual cortices [Hube 59] to facilitate the analysis of visual scenes. Several studies have found support for the hypothesis that the motor control has also a modular organization and does not operate directly with individual muscles.

For Example the study of [Bizz 95] the spinal cords of frogs shows that the stimulation of the interneuronal circuitry leads to a specific balance of muscle activation. They measured mechanical responses of muscles by attaching the frog's limb to a force transducer and electrically stimulating the lumbar spinal cord. The evoked contractions then generate force patterns that direct the frog's limb towards an equilibrium point in space [Muss 00], depicted by Figure 1. A further observation is that the simultaneous stimulation of two sites, each generating a different force field results in the vector sum of the two fields [Bizz 95], thus the force-fields follow the principle of vectorial addition. Such patterns not only serve the CNS to reduce the Degrees of Freedom but the strategy can be applied in the field of robotics in order to reduce the search space for the appropriate drives for a certain motion, what should positively influence the learning of movements. Moreover these

findings build the basic for further hypothesis stating that the modular organization of motor control is based on muscle synergies, which define groups of muscles activated by a single neuronal signal. In the following sections we will cover the different models proposed for muscle synergies, as the synchronous and time-varying synergies. In particular we will focus on the studies of [dAve 05] and [Over 08].

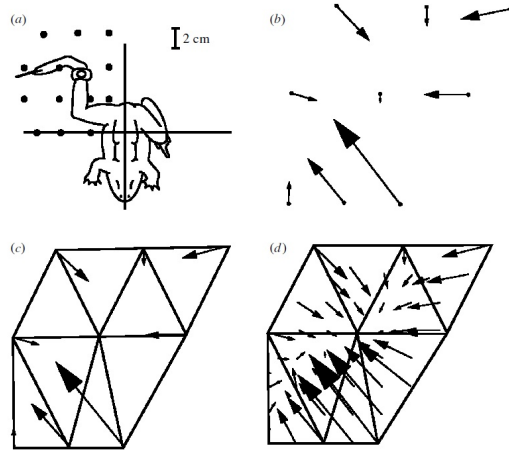


Figure 1: Force field induced by electrical and chemical stimulation of the spinal cord in frogs ([Bizz 95]) (a) The hindlimb was placed at the locations indicated by a by the dots. At each location a stimulus was derived at a fixed site. The resulting force was measured by a force transducer. (b) Force vectors recorded at the nine locations from (a). (c) “The work-space of the hindlimb was partitioned into a set of non-overlapping triangles. Each vertex is a tested point. The force vectors recorded on the three vertices are used to estimate, by linear interpolation, the forces in the interior of the triangle.”[Muss 00] (d) Interpolated force field.

2 Muscle Synergies

The task of finding a muscle combination to perform an appropriate sequence of movements in order to achieve a certain goal turns out to be very complex. As stated above the Degree of Freedom (DOF) Problem must be solved. Many researches have investigated on this topic([dAve 05], [Bizz 95], [Over 08], [Hart 10]), their suggestion is that the central nervous system (CNS) uses a hierarchical structure of muscle modules to simplify motor control. A module can be represented as a set of synergies, which are defined as a set of muscles recruited by a single neural command signal[Torr 06]. So the generation of complex patterns consists of the combination of a few muscle synergies [dAve 05]. The following subsections discuss the representation and characteristics of the different synergy models.

2.1 Synchronous Synergies

A synchronous synergy can be explained as the simultaneous activation of a set of muscles. Such a synergy is represented by [dAve 05] as a vector of real numbers, where each component is one of the simultaneously activated muscles. The muscle activation waveform of each synergy is constructed by scaling each component with an amplitude coefficient c . Finally the muscle pattern is represented by the sum of the generated waveforms.

$$m(t) = \sum_{i=1}^N c_i(t) \times w_i \quad (1)$$

In Equation 1 we can see a muscle pattern $m(t)$ covering P muscles at time t . The amplitude coefficient $c_i(t)$ scales the i th synergy, w_i at time t . If sampled at discrete time intervals Equation 1 results in

$$M = WC. \quad (2)$$

Frog	Behavior	Fraction for each no. of synergies						
		2	3	4	5	6	7	8
F10	Jumping	0.75	0.82	0.86	0.90	0.92	0.94	0.95
F11	Jumping	0.71	0.85	0.89	0.91	0.93	0.95	0.96
F17	Jumping	0.71	0.80	0.86	0.90	0.92	0.94	0.96
F10	Swimming	0.78	0.84	0.89	0.91	0.93	0.95	0.96
F11	Swimming	0.68	0.77	0.82	0.88	0.91	0.94	0.95
F17	Swimming	0.59	0.69	0.76	0.81	0.86	0.90	0.94
F10	Walking	0.56	0.72	0.85	0.89	0.92	0.94	0.96
F11	Walking	0.68	0.79	0.89	0.91	0.94	0.95	0.97
F17	Walking	0.55	0.73	0.80	0.87	0.91	0.93	0.95

Figure 2: Data Variation explained by synchronous synergies [dAve 05]

Where M is a $P \times K$ -matrix, W contains the synergies and C is a $K \times N$ -matrix. In order to reconstruct the data this model requires the adjustment of a large number of parameters, which are represented by C , thus there are $K \times N$ free parameters.

This model covers constant relationships of activation amplitudes as the spatial structure of a muscle pattern. In order to reconstruct the data it requires the adjustment of a large number of parameters, the combination coefficients, which is the total number of samples K times the number of synergies.

In the past years several studies have investigated on the question whether the motor control architecture can be proven to be composed of units like muscle synergies. In most cases techniques like the correlation between muscle pairs met only little success [dAve 02]. Nevertheless an analysis of muscle patterns in frogs using a non-negative matrix factorization algorithm was the first to state support for the hypothesis of muscle synergies ([dAve 05]).

This study investigated the electromyographic activity of 13 hind limb muscles of three adult bull frogs. The electromyographic (EMG) data was collected while the animals were freely jumping or walking in a large cage, or swimming in a tank. Analysis of the extracted synchronous synergies show, that the total variation in the data increased with the number of synergies, ranging from an average 0.67 with two synergies to an average of 0.96 with eight synergies as shown by Figure 2. Thus a great part of the data can be explained with a smaller number of patterns than the dimensionality of the data, which is 13 patterns. To ensure that the algorithm captures real structure the reconstruction error of the extracted synergies was compared to the reconstruction error of synergies obtained from structureless simulated data. The resulting R^2 value of synergies from the real data was significantly higher than the R^2 value based on the simulated data. As the amplitude of each individual muscle was identical in the real and simulated data this implies that the algorithm captures amplitude relationships among muscle activations.

A further comparison of five synergies from the same behaviour of different frogs showed that those synergies were in most cases significantly similar. Indicating that the captured spatial structure does not vary among individuals.

2.2 Time-Varying Synergies

Time-varying synergy is also a term introduced by [dAve 05]. In contrast to synchronous synergies a time-varying synergy is obtained by “scaling different synergies, each sequence multiplied by a single amplitude coefficient, shifting the synergy onset t_i in time, each sequence shifted by a single timing coefficient, and finally summing them muscle by muscle.”[dAve 05] This practice is illustrated by Figure 3 and can be expressed with the following equation as defined by [dAve 02]:

$$m(t) = \sum_{i=1}^N c_i \times w_i(t - t_i) \quad (3)$$

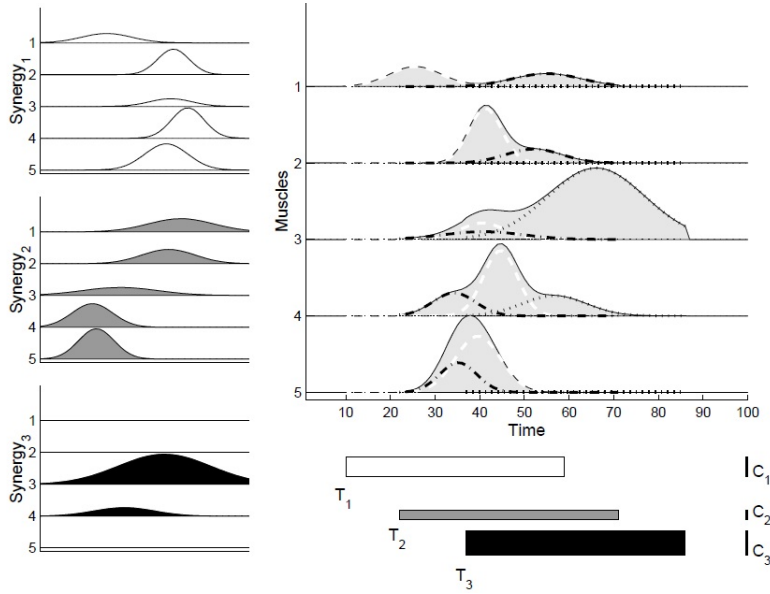


Figure 3: Example of the muscle pattern construction based on three time-varying synergies, taken from [dAve 02]. In this example each time-varying synergy (*left*) is constituted by a sequence of 50 activation levels in 5 muscles chosen as samples from Gaussian functions. The muscle pattern (*top right, shaded*) is constructed by the scaling of by an amplitude coefficient (C_i , represented by the height of the horizontal bars on the *bottom right corner*) and a shift in time (T_i , represented by the position of the bars). At each time step, the components are summed together.

Compared to the synchronous model the pattern $m(t)$ adds the temporal dimension to the previous model and thus covers the spatiotemporal relations. $w_i(\tau)$ is the i th synergy, which is a sequence of P -dimensional vectors representing the P activated muscles at time τ after the synergy onset [dAve 05]. The parameter t_i is the synergy onset and c_i the amplitude coefficient like in Equation 1. If the vectors in the sequence that define the time varying synergy are all of the same direction, this model reduces to the synchronous synergy model.

Regarding the complexity of this model the number of free parameters appears to depend on the amount of instances, where the amplitude and time parameter have to be adjusted. Nevertheless the temporal overlap of different instances of the same synergy is constrained by a refractory period, in general the number of instances of each synergy is less than the number of data samples divided by the number of samples for each synergy (K/Q) [dAve 05]. This means that the number of parameters is $K/Q \times N \times 2$. Where the 2 represent the timing and amplitude coefficient. Despite of the additional dimension the time-varying synergy model requires a lower number of parameters than the synchronous synergy approach. This can be positive, as there are less parameters to control but it can also lead to a less exact data reconstruction as in the case of [Over 08].

The study on muscle synergies analysing muscle activity of the hind limbs of frogs, explained in section 2.1 also analysed time-varying synergies. The goal was to investigate whether muscle synergies are not only based on fixed activation amplitudes but also involve relative muscle activation timings. As for the analysis of synchronous muscle synergies, time-varying synergies were extracted. The variation analysis shows that “the fraction of the total variation in the data explained by the combination of the synergies in each set increased with the number of synergies, ranging from an average R^2 value of 0.65 with two synergies to an average R^2 value of 0.83 with eight synergies” [dAve 05]. Moreover a comparison of the detected spatial structure of five time-varying synergies to the extracted synchronous synergies showed their high similarity. A further investigation on synergies from the same behaviour of different frogs revealed that they are significantly similar, which means that the extracted spatiotemporal synergies are to a large extent similar across the examined animals.

A further research group [Over 08] extended the synergetic model to a particularly complex system, the hand. In addition they analyzed an interesting aspect, the modulation of synergy recruitment by task variables. They collected EMG data of forelimbs from two rhesus macaques while grasping,

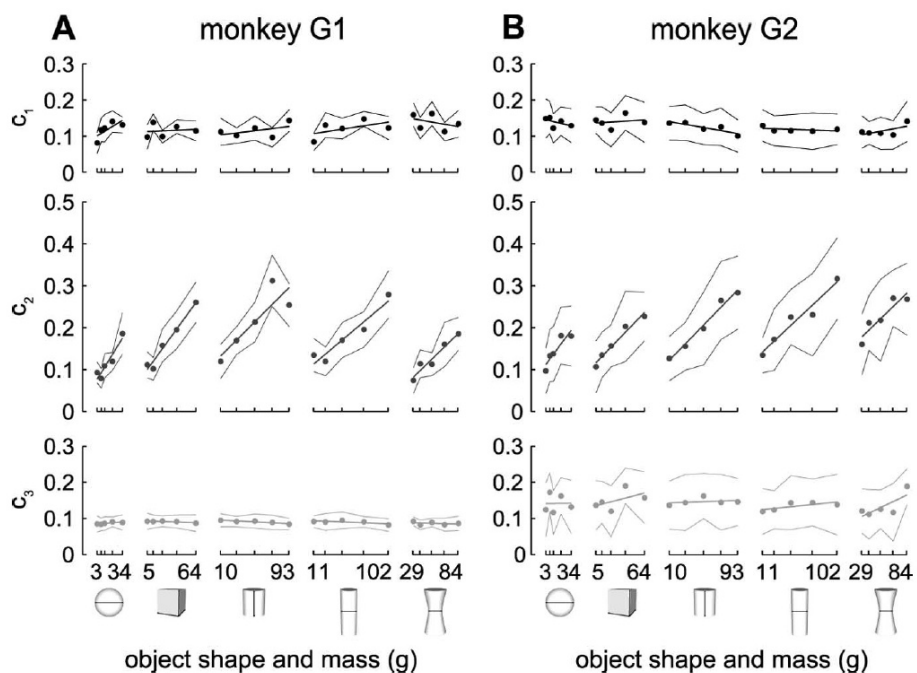


Figure 4: Modulation of synergy amplitude coefficients by object properties (From [Over 08]). A, B, The averaged scaling coefficients from reconstruction of all trials performed by monkey G1 (A) and G2 (B) are plotted versus object shape and size. The object shape is shown at the bottom, whereas the object size is represented as mass along the linear scale for each object. Each point is the average coefficient value across 40 trials in a given object condition thin lines represent one standard deviation. The amplitude of the second synergy c_2 appears to covary particularly strongly with object size.

transportation and release of object of various size and shapes. Synergy extraction was done via an iterative decomposition algorithm using the synergy model defined by Equation 3. The results show that three synergies explained up to 81% of the data variation across 1519 muscles, 100 time points, and 25 object conditions for each monkey. The extracted synergies of one monkey could be uniquely matched to synergies from the other, whereas only two of three exceeded significant similarity. To determine the covariations of each synergy's amplitude and timing coefficient with object shape and size, they “used an analysis of covariance (ANCOVA) in which object mass was the (continuous) predictor and shape was the (discrete) grouping variable of the coefficient data”[Over 08]. This analysis confirmed the observation that especially the c_2 coefficient depends on object size and shape as illustrated by Figure 4, whereas the timing coefficient shows only minor variation for different shapes and sizes.

2.3 Shared and Specific Synergies

The idea of the central nervous system using modular control schemes to cope with the musculoskeletal redundancy and the neural complexity in order to generate movements is widespread. The group of [dAve 05] therefore investigated not only synchronous and time-varying synergies but also whether such synergies are shared between different behaviours. The existence of shared synergies would mean that some synergies are reused in various actions. Implying the reduction of the total number of synergies what also decreases the search space for the appropriate synergy set for a planned task. The following paragraph discusses the synchronous and then the time-varying synergies identified by [dAve 05].

The research on similarities of synchronous synergies in the hind limbs across different behaviours revealed three synergies that are present in walking, jumping and swimming motions of frogs (see Figure 5). Additional synergies were extracted in order to reconstruct each behaviour with five synergies. The reconstruction of the dataset using these synergies resulted in an R^2 value of 0.87 which is essentially similar to that of the episodes of individual behaviour (jumping and swimming

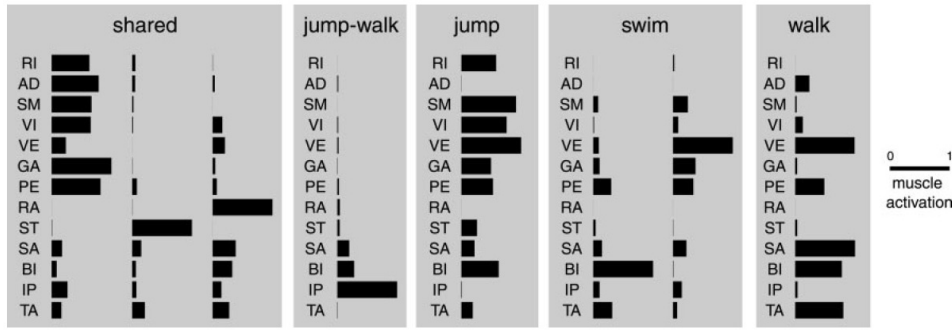


Figure 5: Behavior-independent and behavior-specific synchronous synergies (From [dAve 05]). The three shared synergies are extracted from the entire dataset of muscle patterns recorded during jumping, swimming, and walking in three frogs. One synergy (jump-walk) is extracted from only jumping and walking episodes. The other behavior-specific synergies (jump, swim, and walk) are extracted from only the muscle patterns of individual behaviors. Each synergy is normalized to the maximum over all muscles.

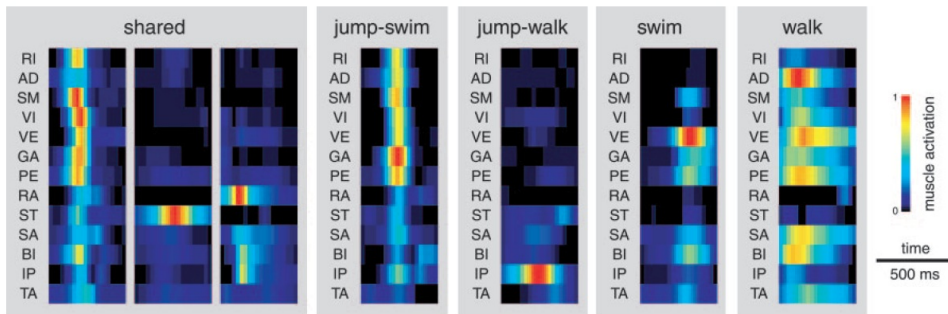


Figure 6: Behaviour-independent and behaviour-specific time-varying synergies (From [dAve 05]). Each synergy represents the activation of the 13 muscles with specific activation waveforms (20 samples for a total duration of 500 ms; amplitude is colour coded) and it is normalized to the maximum over all samples of all muscles. Three shared synergies are extracted from the entire dataset, whereas the other behaviour-specific synergies are extracted from only the muscle patterns from two behaviours (jump-swim and jump-walk) or a single behaviour (swim and walk).

0.86, walking 0.81)[dAve 05]. Thus a set of synchronous shared and specific synergies can reconstruct the data set with a comparable accuracy as synergies extracted from the individual behaviour. The same investigation accomplished for time-varying synergies resulted in three significantly similar pairs across all behaviours and four synergies between jumping and swimming, and jumping and walking, which are depicted by Figure 6. “Each of the three shared time-varying synergies has a spatial organization similar to one of the three synchronous shared synergies while, in addition, possessing distinctive temporal characteristics”[dAve 05]. Concluding, the outcome shows that a set of synchronous and time-varying synergies can be used as units to construct a large repertoire of movements, where some units are shared and others remain specific to certain behaviours.

3 Algorithms for Synergies

Many studies have investigated on the topic of motor control and its modular organization based on muscle synergies. In most cases matrix factorization was used where the observed data is modeled as a linear combination of a small set of basis vectors, as in [dAve 02], [dAve 05], [Hart 10] or [Ivan 06]. In this section we will cover one of this algorithms, the non-negative matrix factorization (NMF) technique used and extended by [dAve 02] and [dAve 05]. We will discuss both, the synergy extraction algorithm of the synchronous and time-varying model.

As defined in Section 2.1 synchronous synergies are represented as the linear combination of non-negative vectors. In order to obtain such synergies out of the recorded EMG data [dAve 05] used

a non-negative matrix factorization algorithm, illustrated by Algorithm 1. It minimizes the total reconstruction error by repeating two steps, consisting of an update of coefficients based on the synergies followed by a further update of the synergies. This is repeated until the reconstruction error gets minimal.

Algorithm 1 Synchronous Synergy Extraction

Initialize the algorithm with random nonnegative synergies (W) and coefficients (C)

Given: W and C

Minimize the reconstruction error:

while Reconstruction Error \geq minimal **do**

$$C_{ij} = C_{ij} \frac{(W^T M)_{ij}}{(W^T W C)_{ij}} \quad \triangleright M \text{ is the muscle pattern from eq. 2}$$

$$W_{ij} = W_{ij} \frac{(M C^T)_{ij}}{(W C C^T)_{ij}} \quad \triangleright \text{Update synergies using the adjusted } C$$

end while

The in Section 2.2 presented time-varying model which expands the previous model by a time dimension, requires another approach for synergy extraction. The time-varying model depends not only on muscle activation amplitudes but also on a relative muscle activation timing, which has to be considered during the synergy extraction. The here presented approach is an extended form of the NMF algorithm, developed by [dAve 02]

Algorithm 2 Reconstruction error minimization

Initialize the algorithm with N random nonnegative synergies (W) and coefficients (C). $\{W_i\}_{i=1\dots N}$, $W_i = [w_i(0)\dots w_i(T-1)]$, $c_{is} (\geq 0) = i$ th coefficient of the episode s

for all episodes s **do**

1. Find the delays t_{ts} as described in Algorithm 3

end for

Update the scaling coefficients c_{si} by gradient descent

for all episodes s **do**

$$2. \Delta c_s = -\mu c \nabla_{c_s} E_s^2$$

end for

Update the synergy elements by gradient descent

for all synergies w_i **do**

$$3. \Delta w_{i\tau} = -\mu w \nabla_{c\tau} E_s^2$$

end for

For a given set of episodes we search for the a set of N non-negative time-varying synergies that minimizes the reconstruction error. As defined in Section 2.2 a synergy $w_i(t)$ is a linear combination of nonnegative vectors representing the activated muscles at the point of time t . The set of coefficients is defined by C , where c_{is} is the i th coefficient for the episode s . Synergies and the coefficients are initialized to non-negative random values and all negative values appearing during computation are substituted by zero. This is due to the always positive nature of muscle activations.

Algorithm 3 Match synergy delays

Initialize the algorithm with N random nonnegative synergies (W) and coefficients (C) $\{W_i\}_{i=1\dots N}$, $W_i = [w_i(0)\dots w_i(T-1)]$, $c_{is} (\geq 0) = i$ th coefficient of the episode s

for all synergies w_i **do**

1. Compute the scalar product cross-correlation at delay t

$$\phi_{si}(t) = \sum_{\tau} m_s(\tau)^T w_i(\tau - t)$$

2. Select synergy and delay with highest cross-correlation

3. Subtract the selected synergy from the data (after scaling and time-shifting by the selected delay).

end for

In order to minimize the reconstruction error the three steps of Algorithm 2 are applied iteratively. At first the delays t_{si} are computed for each episode, given the synergies W_i and coefficients c_{is} . This

is done by a procedure based on cross-correlation, illustrated by Algorithm 3. Once the delays are obtained similar to the Algorithm 1 the scaling coefficients and synergies are updated using gradient descent. It is an optimization algorithm often used to find local minima. In this case it serves to adjust the coefficients and synergies causing a minimal reconstruction error. Which is defined as

$$E^2 = \sum_s E_s^2$$

$$E_s^2 = \sum_{t=1}^{T_s} \left\| m_s(t) - \sum_{i=1}^N c_{si} w_i(t - t_{si}) \right\|^2. \quad (4)$$

According to a study of [Tres 06] comparing different algorithms for synergy extraction like Factor Analysis (FA), Independent Component Analysis (ICA) and NMF on their performance on different data sets, that the NMF algorithms performed similar to the other algorithms regarding the synergy detection and was consistent across data sets.

4 Conclusion

We have seen that even if the CNS controls a large variety of movements with ease, motor control has still a high complexity. A simple movement like the reaching for an object, can be executed in a large amount of different manners. There is possible variation in trajectory, torque and muscle combinations creating a high dimensional search space for the appropriate movement. Several studies, like those of [dAve 02], [Over 08] and [Ivan 06], confirm the hypothesis that motor control has a modular organization. [dAve 05] have found out that these modules consist of muscle synergies which can be represented by two different models, the synchronous or the time-varying synergy model. The synchronous model represents the spatial relationship of activated muscles. The observation of [dAve 02] made clear that several muscles presumed to be part of the same synergy are activated asynchronously, having a slight delay. In order to match those synergies the time-varying model extends the synchronous model by an additional time-dimension.

The results of [dAve 05] on the muscle activity of freely moving intact frogs, show that synchronous synergies are invariant among individuals and even that three synchronous synergies are shared across the considered behaviours jumping, walking and swimming. The analysis of time-varying synergies confirms these results. This indicates that the organization of motor control is highly invariant among individuals and that there must be a hierarchical architecture of synergies, allowing the reuse of basic modules. A further characteristic of the motor control was revealed by [Over 08]. They studied a more complex action, the grasping of monkeys for different objects. The most interesting outcome of their investigation is that certain synergies dependent on size and shape of the objects. [Over 08] suggest that the covariations between synergies and object properties may result from recruitment of invariant muscle synergies, like task parameters.

The here presented studies support the statement that the CNS uses a modular organization of muscles to reduce the complexity of motor control. Their results show that there are modules which can be reused across different behaviours but some modules remain task specific. The modular organization of motor control can be applied to the field of robotics. Especially the reuse of certain models reduces the search space and can improve the flexibility of robotic motion.

References

- [Bizz 95] E. Bizzi, S. Giszter, E. Loeb, F. Mussa-Ivaldi, and P. Saltiel. “Modular organization of motor behavior in the frog’s spinal cord”. *Trends in Neurosciences*, Vol. 18, No. 10, pp. 442–446, 1995.
- [dAve 02] A. d’Avella and M. Tresch. “Modularity in the motor system: decomposition of muscle patterns as combinations of time-varying synergies”. *Advances in neural information processing systems*, Vol. 1, pp. 141–148, 2002.
- [dAve 05] A. d’Avella and E. Bizzi. “Shared and specific muscle synergies in natural motor behaviors”. *Proceedings of the National Academy of Sciences of the United States of America*, Vol. 102, No. 8, p. 3076, 2005.

- [Hart 10] C. Hart and S. Giszter. “A neural basis for motor primitives in the spinal cord”. *The Journal of Neuroscience*, Vol. 30, No. 4, pp. 1322–1336, 2010.
- [Hube 59] D. Hubel and T. Wiesel. “Receptive fields of single neurones in the cat’s striate cortex”. *The Journal of physiology*, Vol. 148, No. 3, pp. 574–591, 1959.
- [Ivan 06] Y. Ivanenko, R. Poppele, and F. Lacquaniti. “Motor control programs and walking”. *The Neuroscientist*, Vol. 12, No. 4, pp. 339–348, 2006.
- [Muss 00] F. Mussa-Ivaldi and E. Bizzi. “Motor learning through the combination of primitives”. *Philosophical Transactions of the Royal Society of London. Series B: Biological Sciences*, Vol. 355, No. 1404, pp. 1755–1769, 2000.
- [Over 08] S. Overduin, A. d’Avella, J. Roh, and E. Bizzi. “Modulation of muscle synergy recruitment in primate grasping”. *The Journal of Neuroscience*, Vol. 28, No. 4, pp. 880–892, 2008.
- [Torr 06] G. Torres-Oviedo, J. Macpherson, and L. Ting. “Muscle synergy organization is robust across a variety of postural perturbations”. *Journal of neurophysiology*, Vol. 96, No. 3, pp. 1530–1546, 2006.
- [Tres 06] M. Tresch, V. Cheung, and A. d’Avella. “Matrix factorization algorithms for the identification of muscle synergies: evaluation on simulated and experimental data sets”. *Journal of Neurophysiology*, Vol. 95, No. 4, pp. 2199–2212, 2006.